Estimation of systolic and diastolic free intracellular Ca^{2+} by titration of Ca^{2+} buffering in the ferret heart

Heide L. KIRSCHENLOHR, Andrew A. GRACE, Jamie I. VANDENBERG, James C. METCALFE and Gerry A. SMITH[1]

Section of Cardiovascular Biology, Department of Biochemistry, University of Cambridge, Tennis Court Road, Cambridge CB2 1QW, U.K.

Spectroscopic Ca^{2+}-indicators are thought to report values of free intracellular Ca^{2+} concentration ($[Ca^{2+}]_i$) that may differ from unperturbed values because they add to the buffering capacity of the tissue. To check this for the heart we have synthesized a new ^{19}F-labelled NMR Ca^{2+} indicator, 1,2-bis-[2-bis-(carboxymethyl)amino-4,5-difluorophenoxy]ethane ('4,5FBAPTA'), with a low affinity (K_d 2950 nM). The new indicator and four previously described ^{19}F-NMR Ca^{2+} indicators 1,2-bis-[2-(1-carboxyethyl)(carboxymethyl)amino-5-fluorophenoxy]ethane ('DiMe-5FBAPTA'), 1,2-bis-[2-(1-carboxyethyl)(carboxymethyl)-amino-4-fluorophenoxy]ethane ('DiMe-4FBAPTA'), 1,2-bis-[2-bis(carboxymethyl)amino-5-fluorophenoxy]ethane ('5FBAPTA') and 1,2-bis-[2-bis(carboxymethyl)amino-5-fluoro-4-methylphenoxy]ethane ('MFBAPTA'), with dissociation constants for Ca^{2+} ranging from 46 to 537 nM, have been used to measure $[Ca^{2+}]_i$, over the range from less than 100 nM to more than 3 μM, in Langendorff-perfused ferret hearts (30 °C, pH 7.4, paced at 1.0 Hz) by ^{19}F-NMR spectroscopy. Loading hearts with indicators resulted in buffering of the Ca^{2+} transient. The measured end-diastolic and peak-systolic $[Ca^{2+}]_i$ were both positively correlated with indicator K_d. The positive correlations between indicator K_d and the measured end-diastolic and peak-systolic $[Ca^{2+}]_i$ were used to estimate the unperturbed end-diastolic and peak-systolic $[Ca^{2+}]_i$ by extrapolation to $K_d = 0$ (diastolic) and to $K_d = \infty$ (systolic) respectively. The extrapolated values in the intact beating heart were 161 nM for end-diastolic $[Ca^{2+}]_i$ and 2650 nM for peak-systolic $[Ca^{2+}]_i$, which agree well with values determined from single cells and muscle strips.

Key words: Ca^{2+} indicators, Ca^{2+}-transient, cardiac, NMR spectroscopy.

INTRODUCTION

The cardiac free intracellular Ca^{2+} concentration ($[Ca^{2+}]_i$) has a critical role in determining myofibrillar contraction [1]. Investigation of the role of $[Ca^{2+}]_i$ has been facilitated by the application of luminescent and fluorescent Ca^{2+} indicators which permit accurate and rapid measurements of $[Ca^{2+}]_i$ [2]. These techniques are generally restricted to use in isolated cardiac myocytes or the superficial cells of multicellular preparations [3]. Unfortunately, it is difficult to correlate the contraction of single cardiac myocytes, which are seldom stress-loaded (e.g. [4,5]), or the superficial cells of perfused hearts, which may not be representative of heart function as a whole [6], with measures of integrated cardiac contractile function.

The $[Ca^{2+}]_i$ in intact hearts can be measured by ^{19}F-NMR spectroscopy using fluorine-labelled Ca^{2+} chelators [7–10]. The advantages of this method include the sensitivity of the ^{19}F nucleus by NMR criteria, the absence of endogenous background ^{19}F-NMR signals [11] and the identification of minor cellular cations such as Zn^{2+} bound to the indicator [12]. In addition, NMR spectra may be obtained without motion artifacts due to cardiac contraction [13]. 1,2-Bis-[2-bis(carboxymethyl)amino-5-fluorophenoxy]ethane (5FBAPTA) has also recently been used to obtain measurements of cardiac $[Ca^{2+}]_i$ *in vivo* [14]. The major disadvantage of the ^{19}F-NMR method is that it requires indicator loading to intracellular concentrations that add significantly to the endogenous cytosolic Ca^{2+}-buffering capacity. This is reflected in perturbations of $[Ca^{2+}]_i$ and a marked decline in left ventricular developed pressure (LVDP) during loading of the indicators [7–10]. For example, the end-diastolic $[Ca^{2+}]_i$ measured with the prototype ^{19}F-NMR indicator, 5FBAPTA, in the perfused ferret heart paced at 1.0 Hz is approx. 500 nM [8], which is significantly higher than the unperturbed diastolic $[Ca^{2+}]_i$ which is thought to be in the range 50–200 nM (reviewed in [1]).

There are currently four ^{19}F-NMR indicators that can be used to measure $[Ca^{2+}]_i$ in intact hearts: 5FBAPTA (K_d 537 nM [11]), 1,2-bis-[2-(1-carboxyethyl)(carboxymethyl)amino-5-fluorophenoxy]ethane (DiMe-5FBAPTA) (K_d 46 nM [15]), 1,2-bis-[2-(1-carboxyethyl)(carboxymethyl)amino-4-fluorophenoxy]ethane (DiMe-4FBAPTA) (K_d 155 nM [15]) and 1,2-bis-[2-bis(carboxymethyl)amino-5-fluoro-4-methylphenoxy]ethane (MFBAPTA) (K_d 270 nM [16]). We have previously shown that the observed $[Ca^{2+}]_i$ in the Langendorff-perfused ferret heart was significantly lower when measured with the high-affinity indicator DiMe-5FBAPTA than with 5FBAPTA [17]. However, when both DiMe-5FBATPA and 5FBAPTA were loaded sequentially into the same heart, the end-diastolic $[Ca^{2+}]_i$ appeared to be determined mainly by the indicator with the lower affinity [17], although the evidence was indirect as the two indicators used could not be resolved spectroscopically. Nevertheless, the data suggest that the buffering properties of the Ca^{2+} indicators can significantly modify $[Ca^{2+}]_i$.

In the present study we have used a new low-affinity Ca^{2+}-indicator, 1,2-bis-[2-bis(carboxymethyl)amino-4,5-difluorophenoxy]ethane (4,5FBAPTA) (K_d 2950 nM), together with the indicators previously synthesized in our laboratory (5FBAPTA, DiMe-4FBAPTA and DiMe-5FBAPTA; see above), as well as MFBAPTA [16], to measure end-diastolic $[Ca^{2+}]_i$ and peak-

Abbreviations used: AM, acetoxymethyl ester; $[Ca^{2+}]_i$, free intracellular Ca^{2+} concentration; DiMe-5FBAPTA, 1,2-bis-[2-(1-carboxyethyl)(carboxymethyl)amino-5-fluorophenoxy]ethane; DiMe-4FBAPTA, 1,2-bis-[2-(1-carboxyethyl)(carboxymethyl)amino-4-fluorophenoxy]ethane; 5FBAPTA, 1,2-bis-[2-bis(carboxymethyl)amino-5-fluorophenoxy]ethane; 4,5FBAPTA, 1,2-bis-[2-bis(carboxymethyl)amino-4,5-difluorophenoxy]ethane; LVDP, left ventricular developed pressure; MFBAPTA, 1,2-bis-[2-bis(carboxymethyl)amino-5-fluoro-4-methylphenoxy]ethane.

[1] To whom correspondence should be addressed (e-mail g.a.smith@bioc.cam.ac.uk).

© 2000 Biochemical Society

systolic $[Ca^{2+}]_i$. The aim was to determine the relationship between the Ca^{2+} affinity of an indicator and the perturbations of apparent end-diastolic $[Ca^{2+}]_i$ and peak-systolic $[Ca^{2+}]_i$, and to determine whether we could estimate the unperturbed diastolic and systolic $[Ca^{2+}]_i$ in the intact beating heart by extrapolation to zero affinity and infinite affinity respectively.

MATERIALS AND METHODS

Synthesis of 4,5FBAPTA

The new indicator, 4,5FBAPTA, was synthesized from 3,4-difluorophenol by similar methods to those described [11,15]. In brief, 3,4-difluorophenol was nitrated with concentrated nitric acid in acetic acid at 5 °C until completion (assayed by TLC on silica developed in chloroform). The reaction mixture was then diluted with water and the crude product was isolated by extraction into petroleum spirit. Pure 2-nitro-4,5-difluorophenol was isolated as a gum from the more polar minor product, 2-nitro-3,4-difluorophenol, by silica gel chromatography in petroleum spirit. Condensation with 1,2-dibromoethane in dimethylformamide, with sodium carbonate, yielded the bis-(4,5-difluoro-2-nitrophenoxy)ethane which was precipitated with water and isolated by filtration (m.p. 138–141 °C). The dinitro compound was reduced in ethanol, with hydrogen, over palladium on charcoal, and the diamine was recovered by filtration and evaporation. Alkylation of the diamine with methyl bromoacetate, in acetonitrile and diisopropylethylamine, gave the tetramethyl ester of 4,5FBAPTA, which was isolated by partitioning into toluene with ammonium phosphate (1 M, pH 3) and purified by silica-gel column chromatography (ethyl acetate/toluene gradient) and crystallization from diethyl ether (m.p. 118–120 °C). The free acid was obtained by hydrolysis with excess NaOH in ethanol followed by dilution with water, acidification with HCl at 5 °C and filtration. The preparation of the tetra-acetoxymethyl ester followed the standard procedure [18].

K_d measurements

The Ca^{2+}-affinity of 4,5FBAPTA was measured by titration at 200–400 nm in 30 mM potassium citrate buffered to pH 7.2 with 40 mM Hepes at 30 °C. Varying proportions of two 10 μM solutions of indicator, one without added Ca^{2+} and the other with a saturating concentration of $CaCl_2$ (20 mM, pH corrected to 7.2), were mixed to determine affinities. The K_d at 30 °C was confirmed by direct titration at 200–400 nm in a 5 cm cuvette of a 1 μM indicator solution with 1 mM $CaCl_2$ in 100 mM KCl/20 mM Hepes without a Ca^{2+} buffer. EGTA (1 mM) was added to a separate sample to determine the zero $[Ca^{2+}]$ spectrum. The basal $[Ca^{2+}]$ and affinity were calculated by iteration [15]. Finally, K_d was also determined by measuring the areas of bound and free NMR signals for various Ca^{2+} concentrations using 100 μM indicator in citrate buffer [15]. All calculations of affinities were iterative and took account of free, bound and basal Ca^{2+} concentrations. For all K_d determinations the slopes of the plots of log([bound indicator]/[free indicator]) against log$[Ca^{2+}]$ were 1.0 ± 0.02. The affinities of hydrolysed samples of acetoxymethyl esters of all the indicators used in this study were the same as for the free acids of the indicators. The addition of up to 1 % (w/v) BSA did not affect indicator K_d, suggesting that any interactions with the protein did not affect the Ca^{2+}-affinity of the indicators. The affinities for a series of heavy metals were also measured by UV titration in citrate buffer using the published affinities of the heavy metals for citrate [19,20].

Heart perfusion

Hearts were prepared as previously described [21,22]. In brief, male ferrets (approx. 6 months old) weighing less than 1.5 kg were anaesthetized with sodium pentobarbitone (250 mg/kg intraperitoneally) (May and Baker Limited, Dagenham, Essex, U.K.) and heparinized (2000 i.u. intraperitoneally) (Sigma Chemicals, Poole, Dorset, U.K.). Hearts were rapidly excised, weighed and arrested in ice-cold perfusion solution (see below). The aorta was cannulated and the heart was Langendorff-perfused at a constant flow rate of 4 ml/min per g wet wt. with a Krebs–Henseleit buffer containing (in mM) 119 NaCl, 4 KCl, 1.8 $CaCl_2$, 1 $MgCl_2$, 25 $NaHCO_3$, 10 glucose and 5 sodium pyruvate, equilibrated to pH 7.4 with O_2/CO_2 (19:1) and maintained at 30 °C.

The atrio-ventricular node was crushed and the heart was paced using square-wave stimuli of 10 ms duration (Grass S48 Stimulator; Grass Instruments Company, Quincy, MA, U.S.A.) at twice the threshold voltage at a rate of 1.0 Hz controlled by the spectrometer [8]. Pacing electrodes were connected to the heart via salt bridges (polythene tubing, internal diam. 1.1 mm, filled with agar saturated with 3 M NaCl) and placed in the right ventricular cavity. LVDP was measured using a fluid-filled latex balloon inserted into the left ventricular cavity connected to a pressure transducer (Spectramed P23XL; Spectramed, Oxnard, CA, U.S.A.). The balloon volume was adjusted to achieve an initial end-diastolic pressure of 10–20 mmHg (1 mmHg = 133.3 Pa). Stimulus pulse, aortic perfusion pressure and LVDP were recorded on a four-channel chart recorder (Gould 2400S; Gould Electronics Limited, Hainault, Essex, U.K.) and tape recorder (model 4S; Racal, Southampton, Hants., U.K.).

The heart was allowed to equilibrate for approx. 90 min, after which the perfusion pressure was routinely 70–80 mmHg. After this period, hearts with a systolic LVP of less than 110 mmHg were rejected. The peak-systolic pressure (means $\pm$ S.D.) in the hearts used was 149 ± 6.0 mmHg at an end-diastolic pressure of 15 ± 1 mmHg ($n = 18$). At the end of each experiment the hearts were blotted dry and weighed (mean heart weight ($\pm$S.D.) 7.9 ± 0.3 g; $n = 18$). The decline in LVDP was less than 15 % over 5 h.

Indicator loading

The ^{19}F-NMR indicators were loaded as cell-permeable acetoxymethyl ester (AM) derivatives. All indicators were made up as 50 mM stock solutions in DMSO. Indicators were loaded into the hearts at a constant rate of 250 μl/h by infusion into the lines carrying the perfusate via a syringe pump, downstream of the bubble trap and filter systems. The perfusate was not recirculated either during the loading or during the following 40 min. Loading was stopped when adequate signal-to-noise (S/N) ratios (more than 10:1) were achieved.

The hydrolysis rates by endogenous esterases of the acetoxymethyl esters of the five indicators varied and determined the time required for indicator loading. Loading was most rapid for 5FBAPTA-AM, with an adequate S/N ratio for the spectrum of 5FBAPTA obtained after 30 min of loading. The other four indicators were hydrolysed more slowly. To increase the rate of hydrolysis, these indicators were mixed in a 2:1 (v/v) ratio with 25 % (w/w) Pluronic F-127 (BASF, Ludwigshafen, Germany) in DMSO before injection into the perfusion line [9,17]. Pluronic F-127 is a non-ionic dispersing agent that helps to solubilize large dye molecules in physiological media [23]. Using this mixture, the loading times were 110 min for 4,5FBAPTA-AM and MFBAPTA-AM, 80 min for DiMe-5FBAPTA-AM and 70 min for DiMe-4FBAPTA-AM. The addition of Pluronic F-127 while

© 2000 Biochemical Society

loading indicators into hearts had no significant effect on LVDP or end-diastolic $[Ca^{2+}]_i$, although end-diastolic pressure was slightly higher (less than 5 mmHg) when Pluronic F-127 was omitted during loading [17]. Hearts were allowed to equilibrate for 40 min following loading of indicators, before the acquisition of data. The concentration of indicator in the cytosolic space is proportional to the area of the ^{19}F-NMR resonances of the indicator and, in a previous paper, using ^{3}H-labelled 5FBAPTA, we showed that, at a S/N ratio of 10:1, the intracellular concentration of 5FBAPTA was 120 μM [21]. All indicators were loaded to similar S/N ratio levels and it was assumed that the final cytosolic concentration of each of the indicators reached approx. 120 μM.

Consecutive loading of indicators

For simultaneous $[Ca^{2+}]_i$ measurements by two indicators, hearts were loaded sequentially with two indicators of different K_d but overlapping titration ranges. In one set of experiments MFBAPTA was loaded for 110 min followed by a 40 min equilibration period and subsequent data collection. Thereafter the lower-affinity indicator, 5FBAPTA, was loaded for 30 min followed by a 40 min equilibration period, and data collection was repeated. In a second set of experiments, DiMe-4FBAPTA was loaded for 70 min plus a 40 min equilibration period followed by perfusion with the high-affinity indicator, DiMe-5FBAPTA, for 80 min plus 40 min of equilibration before NMR measurements were made.

NMR measurements

Hearts were placed in a 9.4 T, 89 mm bore Bruker AM 400 NMR spectrometer, operating at 376 MHz for ^{19}F and equipped with a purpose-built 33 mm diameter probe head as described previously [8]. The magnet was shimmed using the perfusate proton signal: ^{1}H line widths at a half-height of less than 60 Hz were routinely obtained. End-diastolic $[Ca^{2+}]_i$ and the Ca^{2+} transients were obtained using gated pulse sequences as described previously [8,21].

$[Ca^{2+}]_i$ measurements by NMR

The concentration of Ca^{2+}-bound indicator, [bound], and free indicator, [free], are proportional to the area under their respective resonance peaks. The areas under the bound and free resonances were determined by cutting and weighing [8]. $[Ca^{2+}]_i$ measured by each indicator corresponds to the observed signal intensities according to the following equation: $[Ca^{2+}]_i = K_d$[bound]/[free]. All values are reported as means $\pm$ S.D.

RESULTS

K_d measurements

The K_d values for the indicators measured at 30 °C by UV spectroscopy are shown in Table 1. All values were confirmed using NMR spectroscopy and lay within the range $\pm 5\%$ of the values shown in Table 1. Our value for the K_d of MFBAPTA at 30 °C (220 nM, using esterase-hydrolysed AM ester) is consistent with the 270 nM measured at 37 °C by Levy et al. [16].

The ^{19}F-calcium indicators are polyvalent cation chelators and if the ion being chelated is non-paramagnetic the fluoroBAPTAs show unique cation-induced chemical shifts. Where the affinity and the concentration of a cation are appropriate, the fluoroBAPTA will function as an indicator for that cation, for example 5FBAPTA has been used to measure Pb^{2+} [24] and Zn^{2+} [12] in biological tissue. Most importantly for the purposes of this study, the indicators retained selectivity for Ca^{2+} relative to other cations (e.g. DiMe-5FBAPTA: $K_{Ca}/K_{Mg} \approx 10^{-6}$; see Table 2).

NMR chemical shifts

The new indicator, 4,5FBAPTA (Figure 1A), showed two resonances from the Ca^{2+}-bound indicator, which were approximately 2 p.p.m. and 7 p.p.m. downfield from the single peak, corresponding to the two overlapping resonances of the free indicator (Figure 1B). The Ca^{2+}-induced shifts were similar to the shifts of the single fluorine resonances from 4FBAPTA and 5FBAPTA, although the whole spectrum is shifted approximately 26 p.p.m. upfield. NMR spectra for the other indicators have been published previously [11,15,16]. The chemical shifts of the free and bound resonances for all the indicators used are shown in Figure 2.

Relationship between indicator K_d, LVDP and $[Ca^{2+}]_i$

When hearts were loaded with the new indicator, 4,5FBAPTA, there was a marked decrease in peak-systolic pressure and a small increase in end-diastolic pressure. By the time adequate S/N ratios were achieved (more than 10:1) LVDP had decreased to 30 % of the pre-loading LVDP (see Table 1). The end-diastolic $[Ca^{2+}]_i$ measured in hearts loaded with 4,5FBAPTA and paced at 1.0 Hz was 604 ± 29 nM ($n = 3$) and peak-systolic $[Ca^{2+}]_i$ was 2512 ± 210 nM. The corresponding $[Ca^{2+}]_i$ and residual LVDP after loading each indicator are summarized in Table 1.

The end-diastolic $[Ca^{2+}]_i$ increased by more than 3-fold when indicator K_d increased by 60-fold, from 177 ± 21 nM ($n = 14$) when measured with DiMe-5FBAPTA to 604 ± 29 nM ($n = 3$) when measured with 4,5FBAPTA (Figure 3, left panel). For the four higher-affinity indicators (DiMe-5FBAPTA, DiMe-

Table 1 Ca^{2+}-binding properties of ^{19}F-NMR Ca^{2+} indicators

Indicator	K_d at 30 °C (nM)	Titration range (nM)	Loading time (min)	End-diastolic $[Ca^{2+}]_i$ (nM)	n	Systolic $[Ca^{2+}]_i$ (nM)	n	LVDP (% of initial)
4,5FBAPTA	2950	520–17000	110	604 ± 29	3	2512 ± 210	2	30 ± 4
5FBAPTA	537	100–3000	30	522 ± 54	12	1871 ± 123	3	23 ± 2
MFBAPTA	220	40–1100	110	342 ± 24	3	Not determined	–	18 ± 3
DiMe-4FBAPTA	155	30–900	70	265 ± 26	4	706 ± 75	5	9 ± 4
DiMe-5FBAPTA	46	8–300	80	177 ± 21	14	Out of range	–	10 ± 2

© 2000 Biochemical Society

Table 2 Further biophysical characteristics of the indicators

Indicator	Characteristic	Ca^{2+}	Mg^{2+}	H^{+}	Sr^{2+}	Ba^{2+}	Ni^{2+}	Fe^{2+}	Co^{2+}	Mn^{2+}	Zn^{2+}	Cu^{2+}	Cd^{2+}	La^{3+}
5FBAPTA	$\log K_a$			5.85	5.26	5.96	6.88	8.1	8.59	8.76	8.89	12.83	12.96	10.06
	Shift (p.p.m.)	5.6			4.7	3.7	32.6	27.1	31.7	Broad	3.6	Broad	4.9	6.3
DiMe-5FBAPTA	$\log K_a$	7.33	1.94	6.5				7.8			8.6			9.96
	Shift 1 (p.p.m.)	3.96		10.5				16			6.05		3.06	4.58
	Shift 2 (p.p.m.)							6					3.34	5.6
	Shift 3 (p.p.m.)													5.75

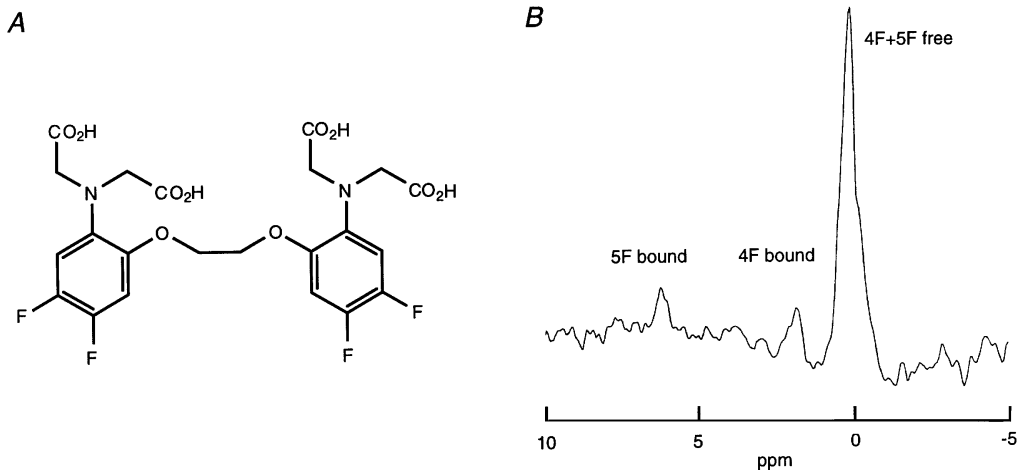

Figure 1 Properties of the new ^{19}F-NMR Ca^{2+} indicator 4,5FBAPTA

(**A**) The structure of 4,5FBAPTA. (**B**) ^{19}F-NMR spectrum obtained at end-diastole from a ferret heart, paced at 1.0 Hz at 30 °C, loaded with 4,5FBAPTA (see the Materials and methods section). The ratio of the Ca^{2+}-bound to free 4,5FBAPTA resonance was 0.17, which represents a $[Ca^{2+}]_i$ of 518 nM.

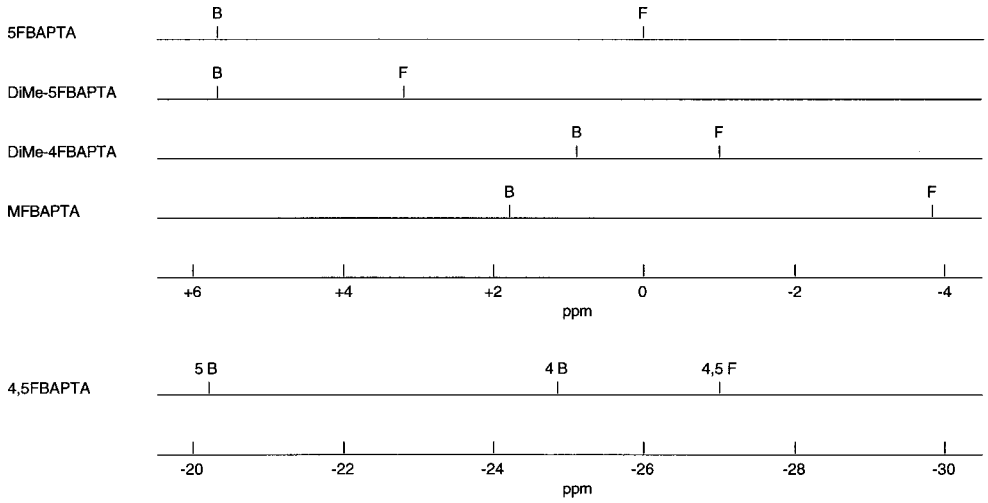

Figure 2 Diagram illustrating the ^{19}F-NMR chemical shifts of the Ca^{2+} indicators loaded into the ferret heart

All the indicators used in this study are in slow NMR exchange with Ca^{2+} at 376 MHz. Chemical shifts are expressed relative to a value of 0 p.p.m. assigned to the resonance of free 5FBAPTA.

4FBAPTA, MFBAPTA and 5FBAPTA) the diastolic $[Ca^{2+}]_i$ measured with each indicator was approximately linearly related to the indicator K_d. Extrapolation of these values to an indicator with zero K_d gives an estimated diastolic $[Ca^{2+}]_i$ of 161 nM. The systolic $[Ca^{2+}]_i$, measured with the lower-affinity indicators, DiMe-4FBAPTA, 5FBAPTA and 4,5FBAPTA, also showed a positive correlation with indicator K_d (Figure 3, right panel). It was not possible to measure the systolic $[Ca^{2+}]_i$ in hearts loaded

© 2000 Biochemical Society

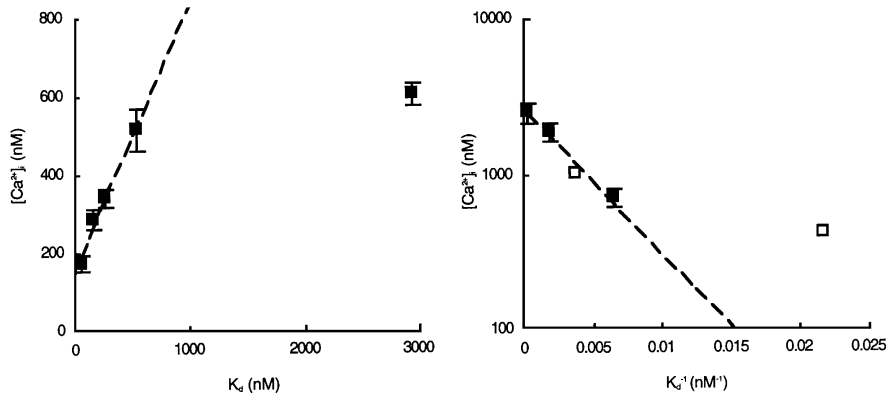

Figure 3 Correlations between indicator K_d and diastolic and systolic $[Ca^{2+}]_i$

Left panel: end-diastolic $[Ca^{2+}]_i$ plotted against the K_d of the indicator used for the $[Ca^{2+}]_i$ measurement. The broken line represents the linear extrapolation used to estimate the unperturbed end-diastolic $[Ca^{2+}]_i$ (see text for details). Right panel: peak-systolic $[Ca^{2+}]_i$ plotted against the affinity ($1/K_d$) of the indicator used for the measurement. The broken line represents the log–linear extrapolation used to estimate the unperturbed peak-systolic $[Ca^{2+}]_i$ (see text for details). The open symbols represent values for peak systolic $[Ca^{2+}]_i$ estimated from cytosolic buffering in the presence of MFBAPTA and DiMe-5FBAPTA because these values could not be measured experimentally. These estimated values were not used in the extrapolations to obtain the unperturbed systolic $[Ca^{2+}]_i$.

with DiMe-5FBAPTA, because at $[Ca^{2+}]_i > 400$ nM the area of the free peak was too small to be distinguished from noise. The plot of systolic $[Ca^{2+}]_i$ against indicator affinity is pseudo-exponential and as the affinity approaches zero the value of the systolic $[Ca^{2+}]_i$ approaches 2650 nM (broken line, Figure 3, right panel).

Effect of indicator co-loading on end-diastolic $[Ca^{2+}]_i$

Effective co-loading experiments require indicators whose free and Ca^{2+}-bound resonances do not coincide but whose titration ranges overlap sufficiently to enable accurate $[Ca^{2+}]_i$ measurements with both indicators [16,17]. From the ^{19}F-NMR chemical shifts of the five indicators loaded in perfused ferret hearts (Figure 2) and the K_d values in Table 1, the indicator pairs 5FBAPTA with MFBAPTA and DiMe-5FBAPTA with DiMe-4FBAPTA were selected as suitable for co-loading experiments (see Figure 4).

In the first set of experiments MFBAPTA was loaded before 5FBAPTA (Figure 4, left panel). MFBAPTA alone gave an end-diastolic $[Ca^{2+}]_i$ of 327 ± 24 nM ($n = 3$), but after the loading of 5FBAPTA into the same heart, the end-diastolic $[Ca^{2+}]_i$ increased significantly to 439 ± 15 nM, measured with MFBAPTA, or 534 ± 31 nM ($n = 3$), measured with 5FBAPTA. The latter value is comparable to the end-diastolic value of 522 ± 54 nM ($n = 12$) measured in hearts loaded with 5FBAPTA alone. In the second series of experiments DiMe-4FBAPTA was loaded before DiMe-5FBAPTA (Figure 4, right panel). DiMe-4FBAPTA alone reported an end-diastolic $[Ca^{2+}]_i$ of 265 ± 45 nM ($n = 4$). Loading DiMe-5FBAPTA into the same heart did not change the end-diastolic $[Ca^{2+}]_i$ measured with DiMe-4FBAPTA, i.e. 275 ± 40 nM. The end-diastolic $[Ca^{2+}]_i$ measured with DiMe-5FBAPTA was 204 ± 32 nM ($n = 4$, $P < 0.05$ compared with the value measured in hearts loaded with DiMe-5FBAPTA alone, i.e. 171 ± 21 nM, $n = 9$).

DISCUSSION

Buffering effects of indicator

Ideally, the K_d of an indicator should be close to the $[Ca^{2+}]_i$ to be measured, as this will optimize sensitivity in the system [25]. With regard to ^{19}F-NMR indicators, changes in $[Ca^{2+}]_i$ near the K_d of the indicator will cause larger, and therefore more easily measurable, changes in the areas of the NMR resonances. Thus we were able to obtain measurements of end-diastolic $[Ca^{2+}]_i$ by using indicators with K_d values in the range 46–2950 nM at 30 °C but we were only able to measure peak-systolic $[Ca^{2+}]_i$ by using indicators with K_d values of at least 155 nM (see Table 1). These considerations suggest that 5FBAPTA (K_d 537 nM at 30 °C) would be an appropriate indicator for measuring both diastolic and systolic $[Ca^{2+}]_i$. However, if the cytosolic concentration of the indicator is high relative to the amount of Ca^{2+} mobilized during the Ca^{2+} transient, the indicator will bind an appreciable portion of the mobilized Ca^{2+}. Hence the change in $[Ca^{2+}]_i$ during the transient will be diminished by the added buffer, or extra Ca^{2+} will be mobilized to negate this effect. The results in this study suggest that in the perfused heart the dominant effect is that the change in free $[Ca^{2+}]_i$ during the transient is reduced by the added buffer (see Table 1).

In this study all indicators were loaded to similar levels, approx. 120 μM (see the Materials and methods section). Under these conditions the data show that the buffering effect of the indicators was K_d-dependent. The end-diastolic $[Ca^{2+}]_i$ was increased by the presence of an indicator and this increase was approximately linearly related to the indicator K_d (see Figure 3, left panel), whereas the peak-systolic $[Ca^{2+}]_i$ was reduced by the presence of the indicator with the peak-systolic $[Ca^{2+}]_i$ decreasing with decreasing indicator K_d (see Figure 3, right panel). These empirical relationships suggested that we could use the data to extrapolate the unperturbed end-diastolic and peak-systolic $[Ca^{2+}]_i$. The extrapolations used were based on the relationships between $[Ca^{2+}]_i$ and indicator K_d as illustrated in Figure 5. The experimental data (Figure 3) show that an added buffer with a K_d in the range of the cardiac $[Ca^{2+}]_i$ transient raises end-diastolic $[Ca^{2+}]_i$ and reduces peak-systolic $[Ca^{2+}]_i$ (illustrated by the solid lines in Figure 5). If the added buffer has a very low affinity (K_d much greater than peak-systolic $[Ca^{2+}]_i$) it will have negligible effect on $[Ca^{2+}]_i$ because little Ca^{2+} will be bound to the indicator in either diastole or systole (broken lines in Figure 5). Conversely, if the added buffer has very high affinity (K_d much less than end-diastolic $[Ca^{2+}]_i$) it will be totally bound in diastole and therefore cannot bind any additional Ca^{2+} during systole and so will have

© 2000 Biochemical Society

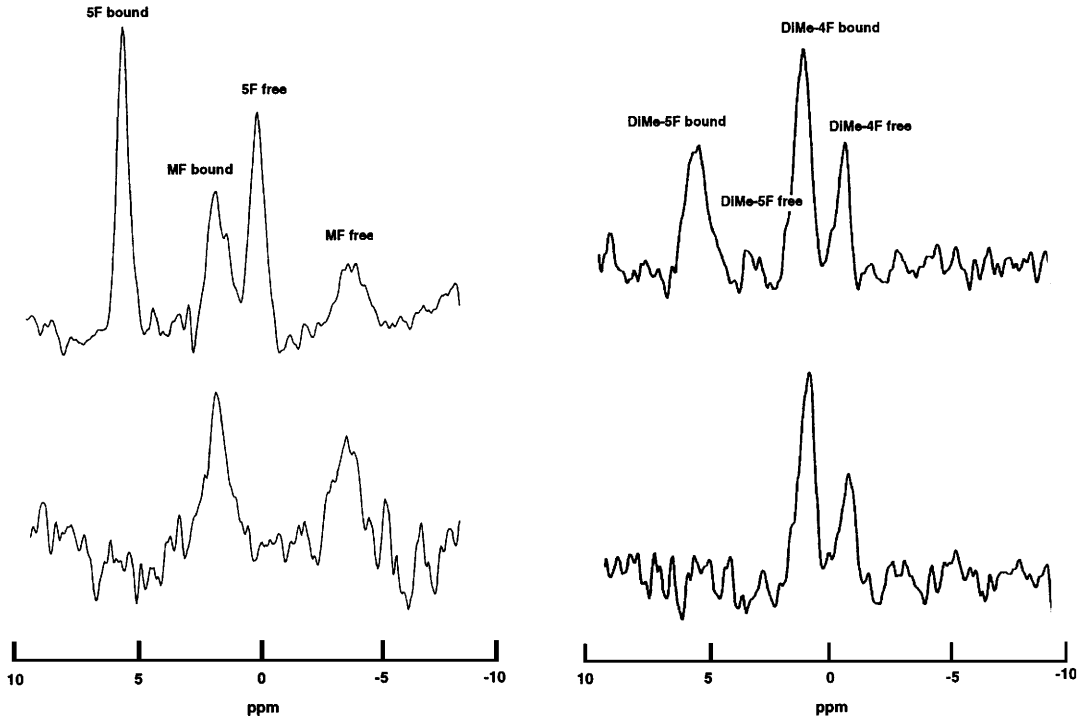

Figure 4 ^{19}F-NMR obtained from ferret heart after co-loading with the Ca^{2+} indicators

Left panel: ^{19}F-NMR spectra obtained from a ferret heart co-loaded with 5FBAPTA after MFBAPTA. Right panel: ^{19}F-NMR spectra obtained from a ferret heart co-loaded with DiMe-5FBAPTA after DiMe-4FBAPTA.

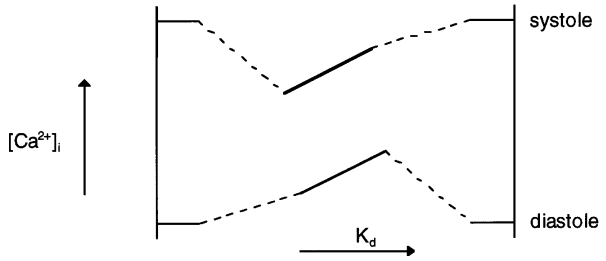

Figure 5 Diagram illustrating the effect of varying the K_d of an exogenous Ca^{2+} buffer on the Ca^{2+} transient

Indicators with very high affinity will be fully bound during both diastole and systole and so will not buffer the cardiac Ca^{2+} transient. Conversely, indicators with very low affinity will not bind Ca^{2+} during diastole or systole and so will not buffer the cardiac Ca^{2+} transient. Between these points, however, the buffering of the cardiac Ca^{2+} transient is dependent on the indicator K_d.

negligible influence on $[Ca^{2+}]_i$. This implies that between the extremes of very high and very low K_d there must be inflections in the plot of measured $[Ca^{2+}]_i$ against indicator K_d (dotted lines in Figure 5). The inflections occur on the higher-affinity (low K_d) side for the systolic $[Ca^{2+}]_i$ and on the lower-affinity (high K_d) side for the diastolic $[Ca^{2+}]_i$. Therefore extrapolating to $K_d = 0$ will give an estimate of the diastolic $[Ca^{2+}]_i$ and extrapolating to $K_d = \infty$ will give an estimate of the systolic $[Ca^{2+}]_i$.

A linear function was used to extrapolate diastolic $[Ca^{2+}]_i$ and a log–linear function to extrapolate systolic $[Ca^{2+}]_i$, as these were the simplest functions that fitted the data empirically. From Figure 5 it is apparent that the extrapolations used would lead to an underestimation of the diastolic $[Ca^{2+}]_i$ and an overestimation of the systolic $[Ca^{2+}]_i$. However, the extrapolated value for the diastolic $[Ca^{2+}]_i$, 161 nM, was within the error range of the diastolic $[Ca^{2+}]_i$ measured with the highest-affinity indicator (171 ± 21 nM, DiMe-5FBAPTA) and the extrapolated value for systolic $[Ca^{2+}]_i$, 2650 nM, was within the error range of the systolic $[Ca^{2+}]_i$ measured with the lowest-affinity indicator (2510 ± 210 nM, 4,5FBAPTA). Therefore the extrapolation function used does not appear to be a significant source of error in the estimation of the unperturbed $[Ca^{2+}]_i$ compared with the S.D. of 8–11 % for the experimental $[Ca^{2+}]_i$ measurements. Furthermore, our estimate of end-diastolic $[Ca^{2+}]_i$ agrees well with values obtained using fluorescent indicators in isolated myocytes (e.g. [26,27]) and muscle strips (e.g. [28,29]). Our estimate of peak-systolic $[Ca^{2+}]_i$ is similar to the values reported from experiments using aequorin, a low-affinity, high-sensitivity indicator (e.g. [30]), but is higher than most values reported from experiments using fluorescent indicators. It is likely, however, that the buffering properties of the fluorescent indicators means that most reported values are perturbed rather than true peak-systolic values, as has been clearly demonstrated by, for example, Wier and co-workers [27], and modelled by Noble and Powell [31].

Simultaneous end-diastolic $[Ca^{2+}]_i$ measurements

From Figure 3 (left panel) it is apparent that the lower-affinity indicators cause more perturbation of the diastolic $[Ca^{2+}]_i$ than higher-affinity indicators. When two indicators are loaded to similar concentrations we would therefore expect that the diastolic $[Ca^{2+}]_i$ should be closer to the value measured in the

© 2000 Biochemical Society

presence of the lower-affinity indicator alone. The end-diastolic $[Ca^{2+}]_i$ measured by MFBAPTA was significantly increased from 324 ± 24 to 439 ± 15 nM following loading of a lower-affinity indicator, 5FBAPTA. Similarly, the end-diastolic $[Ca^{2+}]_i$ measured by DiMe-5FBAPTA was increased from 171 ± 21 to 204 ± 32 nM when measured in the presence of the lower-affinity indicator DiMe-4FBAPTA. In both sets of experiments the end-diastolic $[Ca^{2+}]_i$ measured by the lower-affinity indicator was not significantly affected by co-loading a higher-affinity indicator.

Despite the limitations of the co-loading experiments, the data are consistent with the predicted effect of loading two indicators with different K_d values. Furthermore, the similarity of the $[Ca^{2+}]_i$ measured with both indicators in the co-loading experiments suggests that the relative K_d values measured by UV or NMR spectrometry *in vitro* are very similar to the relative K_d values *in vivo* and that the indicators load into the same cell compartment. The differences in end-diastolic $[Ca^{2+}]_i$ reported by the different indicators are therefore a direct result of their K_d values.

We thank Mr. David Reed for excellent technical assistance. The work was supported by the Medical Research Council and a British Heart Foundation project grant. A.A.G. is a British Heart Foundation Senior Research Fellow (FS/97026) and J.I.V. is a British Heart Foundation Basic Science Lecturer (BS/9502). MFBAPTA-AM ester was a gift from Dr. R. E. London (Duke University, Durham, NC, U.S.A.)

REFERENCES

1 Bers, D. (1991) Excitation Contraction Coupling and Cardiac Contractile Force, Kluwer Academic Publishers, Dordrecht
2 Blinks, J. (1991) in The Heart and Cardiovascular System (Fozzard, H., Haber, E., Jennings, R., Katz, A. and Morgan, H., eds.), pp. 1171–1203, Raven Press, New York
3 Lee, H. C., Smith, N., Mohabir, R. and Clusin, W. T. (1987) Proc. Natl. Acad. Sci. U.S.A. **84**, 7793–7797
4 O'Rourke, B., Reibel, D. K. and Thomas, A. P. (1990) Am. J. Physiol. **259**, H230–H242
5 Spurgeon, H. A., Stern, M. D., Baartz, G., Raffaeli, S., Hansford, R. G., Talo, A., Lakatta, E. G. and Capogrossi, M. C. (1990) Am. J. Physiol. **258**, H574–H586
6 Lorell, B. H., Apstein, C. S., Cunningham, M. J., Schoen, F. J., Weinberg, E. O., Peeters, G. A. and Barry, W. H. (1990) Circ. Res. **67**, 415–425
7 Metcalfe, J. C., Hesketh, T. R. and Smith, G. A. (1985) Cell Calcium **6**, 183–195
8 Kirschenlohr, H. L., Metcalfe, J. C., Morris, P. G., Rodrigo, G. C. and Smith, G. A. (1988) Proc. Natl. Acad. Sci. U.S.A. **85**, 9017–9021
9 Marban, E., Kitakaze, M., Kusuoka, H., Porterfield, J. K., Yue, D. T. and Chacko, V. P. (1987) Proc. Natl. Acad. Sci. U.S.A. **84**, 6005–6009
10 Steenbergen, C., Murphy, E., Levy, L. and London, R. E. (1987) Circ. Res. **60**, 700–707
11 Smith, G. A., Hesketh, R. T., Metcalfe, J. C., Feeney, J. and Morris, P. G. (1983) Proc. Natl. Acad. Sci. U.S.A. **80**, 7178–7182
12 Kirschenlohr, H., Grace, A., Shachar Hill, Y., Metcalfe, J., Morris, P. and Smith, G. (1990) Proc. Soc. Magn. Reson. Med. **9**, 900
13 Smith, G. and Bachelard, H. (1994) Methods Neurosci. **27**, 153–195
14 Song, S. K., Hotchkiss, R. S., Neil, J., Morris, Jr., P. E., Hsu, C. Y. and Ackerman, J. J. (1995) Am. J. Physiol. **269**, C318–C322
15 Clarke, S., Metcalfe, J. and Smith, A. (1993) J. Chem. Soc. Perkin Trans. 2 1187–1194
16 Levy, L. A., Murphy, E. and London, R. E. (1987) Am. J. Physiol. **252**, C441–C449
17 Kirschenlohr, H. L., Grace, A. A., Clarke, S. D., Shachar-Hill, Y., Metcalfe, J. C., Morris, P. G. and Smith, G. A. (1993) Biochem. J. **293**, 407–411
18 Tsien, R. Y. (1981) Nature (London) **290**, 527–528
19 Martell, A. and Smith, R. (1994) Critical Stability Constants, vol. 1, Plenum Press, New York
20 Martell, A. and Smith, R. (1997) Critical Stability Constants, vol. 3, Plenum Press, New York
21 Harding, D. P., Smith, G. A., Metcalfe, J. C., Morris, P. G. and Kirschenlohr, H. L. (1993) Magn. Reson. Med. **29**, 605–615
22 Grace, A. A., Kirschenlohr, H. L., Metcalfe, J. C., Smith, G. A., Weissberg, P. L., Cragoe, Jr., E. J. and Vandenberg, J. I. (1993) Am. J. Physiol. **265**, H289–H298
23 Poenie, M., Alderton, J., Steinhardt, R. and Tsien, R. (1986) Science **233**, 886–889
24 Schanne, F. A., Dowd, T. L., Gupta, R. K. and Rosen, J. F. (1989) Proc. Natl. Acad. Sci. U.S.A. **86**, 5133–5135
25 Tsien, R. Y. (1980) Biochemistry **19**, 2396–2404
26 Trafford, A. W., Diaz, M. E., O'Neill, S. C. and Eisner, D. A. (1995) J. Physiol. (London) **488**, 577–586
27 Balke, C. W., Egan, T. M. and Wier, W. G. (1994) J. Physiol. (London) **474**, 447–462
28 Backx, P. H. and Ter Keurs, H. E. (1993) Am. J. Physiol. **264**, H1098–H1110
29 Lamont, C. and Eisner, D. A. (1996) Pflugers Arch. **432**, 961–969
30 Kihara, Y., Grossman, W. and Morgan, J. P. (1989) Circ. Res. **65**, 1029–1044
31 Noble, D. and Powell, T. (1991) Proc. R. Soc. Lond. B **246**, 167–172

Received 17 September 1999/10 November 1999; accepted 2 December 1999

© 2000 Biochemical Society